HAL
archives-ouvertes.fr

Single-Event-Transient Effects in Junctionless Double-Gate MOSFETs with Dual-Material Gate Investigated by 3D Simulation

Daniela Munteanu, Jean-Luc Autran, Soilihi Moindjie

▶ To cite this version:

Daniela Munteanu, Jean-Luc Autran, Soilihi Moindjie. Single-Event-Transient Effects in Junctionless Double-Gate MOSFETs with Dual-Material Gate Investigated by 3D Simulation. 28th European Symposium on Reliability of Electron Devices, Failure Physics and Analysis (ESREF 2017), Sep 2017, Bordeaux, France. hal-01787612

HAL Id: hal-01787612
https://hal-amu.archives-ouvertes.fr/hal-01787612

Submitted on 7 May 2018

HAL is a multi-disciplinary open access archive for the deposit and dissemination of scientific research documents, whether they are published or not. The documents may come from teaching and research institutions in France or abroad, or from public or private research centers.

L'archive ouverte pluridisciplinaire HAL, est destinée au dépôt et à la diffusion de documents scientifiques de niveau recherche, publiés ou non, émanant des établissements d'enseignement et de recherche français ou étrangers, des laboratoires publics ou privés.

Single-Event-Transient Effects in Junctionless Double-Gate MOSFETs with Dual-Material-Gate investigated by 3D Simulation

D. Munteanu[a], J.L. Autran[a,*], S. Moindjie[a]

[a] *Aix-Marseille University & CNRS, IM2NP (UMR 7334), Faculté des Sciences – Service 142, Avenue Escadrille Normandie Niémen, F-13397 Marseille Cedex 20, France*

Abstract

The Junctionless Double-Gate MOSFET combined with a Dual-Material Gate (JL-DMDG) is interesting for future ultra-scaled devices thanks to a simplified technological process (no junctions), reduced leakage currents and capability to reduce SCEs and HCEs (due to the step in the potential profile). In this work, we investigate the bipolar amplification and charge collection in JL-DMDG submitted to heavy-ion irradiation. We show that JL-DMDG is more sensitive to radiation than more conventional devices with single-material-gate or operating in inversion-mode.

***Corresponding author.**
jean-luc.autran@univ-amu.fr
Tel: + 33 (0)413 594 627; Fax: +33 (0)491 288 531

Single-Event-Transient Effects in Junctionless Double-Gate MOSFETs with Dual-Material-Gate investigated by 3D Simulation

D. Munteanu[a], J.L. Autran[a,*], S. Moindjie[a]

1. Introduction

Double-Gate (DG) MOSFET technology is recognized as a promising solution to meet the roadmap requirements in the nanometre scale, namely due to its excellent control of short channel effects (SCE) ensured by the presence of an additional gate electrode which enhance the potential control of the channel [1]. The DG MOSFET technological process can be simplified by using a junctionless (JL) structure [2-3], with the same type of semiconductor throughout the entire silicon film (Fig. 1a). This device has some interesting advantages: there is no doping concentration gradients in the device and the junction leakage currents are totally suppressed, so the off-state current is uniquely controlled by the gate which could be very attractive for ultra-scaled devices. Another interesting concept is to use a dual-material-gate (DM) in order to reduce the hot-carrier induced effects (HCE) and drain-induced barrier lowering (DIBL) phenomena [4]. The junctionless DG MOSFET with dual-material-gate (JL-DMDG) has two materials in the gates (Fig. 1b), with different workfunctions, Φ_{M1} and Φ_{M2}. This configuration induces a step in the surface-potential profile (see Fig. 2) which, for $\Phi_{M1}>\Phi_{M2}$, simultaneously provides transconductance increase and DIBL reduction. The step function profile of the surface potential ensures screening of the channel region on the source side (under the material M1) from drain-potential variations. In addition, the electric field peak at the drain is considerably reduced, which suppresses HCEs [5-6]. JL-DMDG is then a promising structure for which extensive modelling works have been reported in the literature [7-8] in the last years. However, at the best of our knowledge, radiation-sensitivity studies of these devices have not been performed. In this paper we investigate by 3-D numerical simulation the response to single-event of JL-DMDG through a detailed comparison with more usual inversion-mode (IM-DMDG [9], Fig. 1c) and

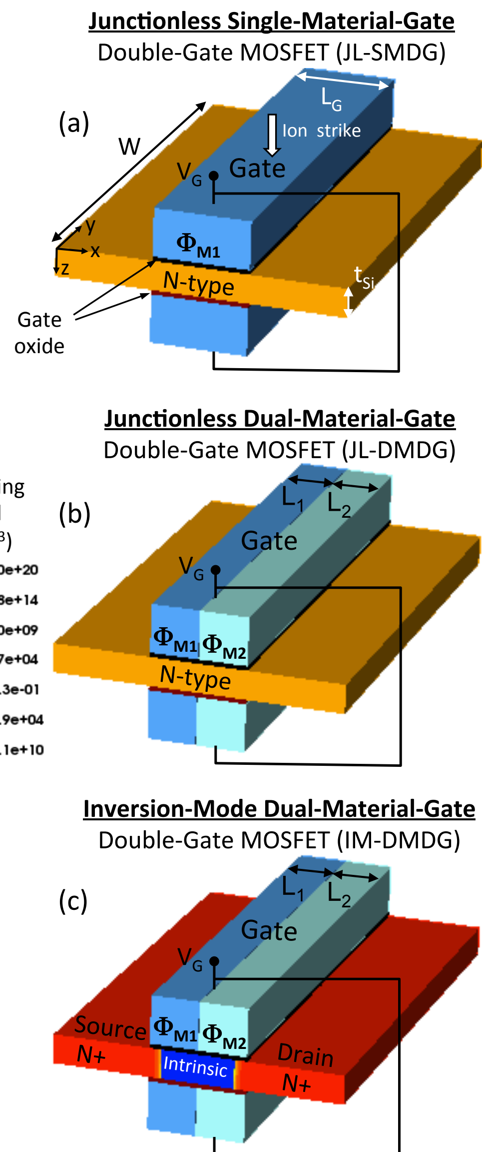

Fig. 1. Schematic description of the simulated symmetrical JL-SMDG, JL-DMDG and IM-DMDG devices. For a better view, spacers and isolation oxides are not shown.

* Corresponding author: jean-luc.autran@univ-amu.fr.

single-material-gate devices (JL-SMDG [10] and IM-SMDG [11]). The impact of several technological parameters on single-event transients and bipolar amplification is also addressed.

2. Simulated devices and models

Four types of devices have been considered: JL-DMDG, IM-DMDG, JL-SMDG and IM-DMDG. All devices are designed with the same geometrical dimensions: channel length L_G=20 nm, 100 nm gate width, 6 nm-thick silicon film and 1 nm-thick gate oxide, similar to real devices reported in [12]. In junctionless devices, the entire silicon film is uniformly n-type doped at 10^{19} cm^{-3}. The inversion-mode devices (IM-DMDG and IM-SMDG) have an intrinsic channel; source and drain regions are highly n-type doped and the doping profile in these regions is uniform. In single-gate devices (JL-SMDG and IM-SMDG), a single-material M1 is used for the gates. In dual-material-gate devices (JL-DMDG and IM-DMDG) the gates consists of dual materials, M1 (Φ_{M1}) and M2 (Φ_{M2}), of lengths L_1 and L_2, respectively (L_1+L_2=L_G). In a first time we considered L_1=L_2=L_G/2, Φ_{M1}=4.8 eV and Φ_{M2}=4.1 eV.

3-D numerical simulations have been performed with the DESSIS device simulator from Synopsis Inc. [13]. The main models used in simulation are the Shockley-Read-Hall and Auger recombination models, the Fermi-Dirac carrier statistics and the hydrodynamic model was used for the carrier transport equations. The impact ionization model depends on carriers energy. The mobility model includes the dependence on the carrier energy, lattice temperature and doping level. The ion strike was simulated using the DESSIS HeavyIon module [13]. The electron-hole pair column created in the device by the ion strike is modeled using a carrier-generation function which has a Gaussian radial distribution with a characteristic radius of 20 nm, a Gaussian time distribution, centered on 10 ps and having a characteristic width of 2 ps. In a first time, the ion strikes in the channel center (x=30nm). Other hit locations will be considered next. Devices are biased in the off state (V_G=0V). The drain is constantly biased at a power supply voltage equal to 1 V.

3. Static characteristics

The surface potential profile in junctionless and inversion mode devices is plotted in Figure 2. As expected, the surface potential in dual-material-gate devices has a step-function profile, which is not present for single-material gate devices. This step function profile is responsible of DIBL reduction and transconductance enhancement. The simulated steady-state drain current characteristics of JL-DMDG, IM-DMDG, JL-SMDG and IM-DMDG are plotted in Fig. 3. Single-material-gate devices have lower off-state current than their dual-material-gate counterparts and near ideal subthreshold swings (63 mV/dec). JL-DMDG device has the higher off-state current but lower subthreshold swing (71 mV/dec) than the IM-DMDG device (83.3 mV/dec). Junctionless devices exhibit lower on-state current than inversion-mode devices because the highly doped silicon film degrades the mobility [10].

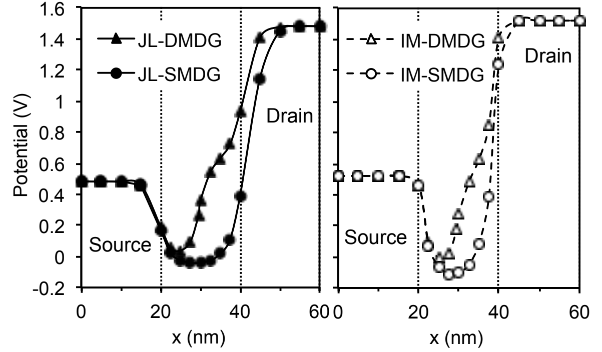

Fig. 2. Surface potential profiles at V_G=0V and V_D=1V.

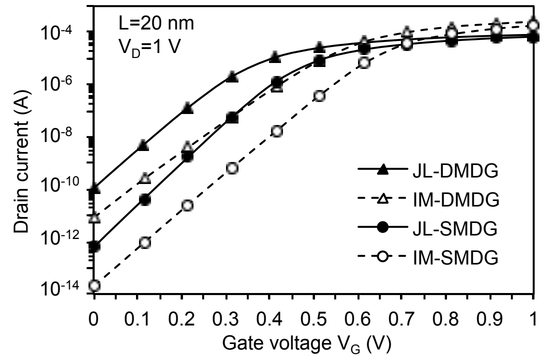

Fig. 3. Drain current as function of gate voltage at V_D=1V.

4. Single-Event-Induced Transients

4.1. Drain current transient

Figure 4 shows the drain current transient resulting from an ion hit in the channel center of the simulated devices, the ion having a linear energy transfer (LET) of 0.1 MeV.cm^2/mg. The highest drain current transient peak is obtained for JL-DMDG device. Dual-material-gate device have higher transient peaks and wider transients that single-

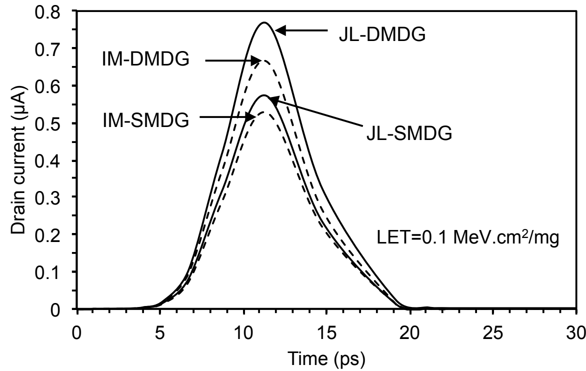

Fig.4. Drain current transients for an ion hit in the center of the channel (LET=0.1 MeV.cm^2/mg).

material gate devices. The reason is probably a higher bipolar gain for dual-material-gate devices due to the step-function profile of the channel potential.

4.2. Collected charge and bipolar amplification

Figures 5a and 5b show the variation of the collected charge (Q_{COLL}) and bipolar amplification as function of LET. Q_{COLL} is obtained by integrating the simulated drain current over the transient duration. The deposited charge, Q_{DEP}, is calculated considering the Gaussian distribution of the ion track and the exact 3-D geometry of the silicon body. The bipolar gain is then given by the ratio between the Q_{COLL} and Q_{DEP}. The LET range considered here corresponds to the LET range of a neutron-induced ion in silicon in the terrestrial environment [14]. Dual-material-gate devices have higher parasitic bipolar amplification than the single-material-gate counterparts. This can be explained by the reduction of the effective channel length in dual-material-gate devices induced by the presence of a gate material with lower workfunction on the drain side of the gate, which induces a step-function potential profile. Then the collected charge and the bipolar gain values are higher in these devices than those obtained in single-material-gate devices. Concerning the dual-material-gate devices, JL-DMDG exhibits a higher bipolar gain than IM-DMDG because of more important floating body effects in the channel of the junctionless device having a higher doping level than the channel of inversion-mode device which is intrinsic. The difference between the four devices is important at low LET, but it gradually weakens when the LET increases. The explanation is that at high LET the electric field is collapsed and then potential variations in the channel have less impact on the parasitic bipolar amplification. The bipolar gain then becomes nearly the same for all devices.

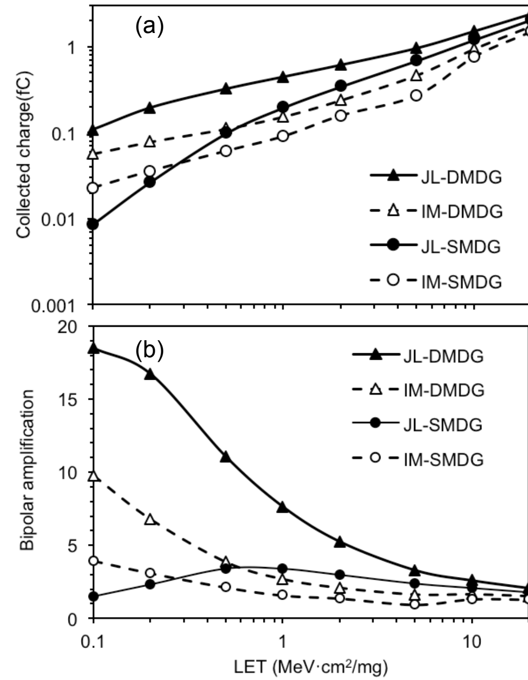

Fig. 5. Collected charge and bipolar amplification as function of LET for an ion hit in the center of the channel.

4.3. Device sensitivity to ion hit location

We consider in the following different ion hit locations along the x-axis between the source contact (x=0) and the drain contact (x=60 nm). The drain current peak (Fig. 6) and the transient width increase as the ion strike location moves from source to drain with a maximum value at x=40 nm for LET=10 MeV.cm^2/mg. The collected charge and the bipolar gain as a function of the strike location are shown in Fig. 7. The deposited charge, $Q_{DEP,}$ is also reported for comparison. Q_{DEP} is highest in the middle of the channel and decreases toward the source and drain sides of the silicon film, because a reduced part of the ion track is contained in the active region [10]. Q_{COLL} has a bell-shaped profile with a maximum at x=40 nm. For all x locations Q_{COLL} is higher in junctionless than in inversion-mode devices. For ion strikes in the source of IM-DMDG and IM-SMDG, Q_{COLL} is lower than Q_{DEP}. This indicates that the bipolar amplification (Fig. 7b) is very low and that there is a strong recombination of the deposited charge in the device [10]. The bipolar gain is always higher in junctionless than in inversion-mode devices, but has similar dependences on ion hit location for the four structures. The bipolar gain maximum is located at the channel-drain junction in IM-DMDG and IM-SMDG and at x=50 nm for JL-DMDG and JL-SMDG.

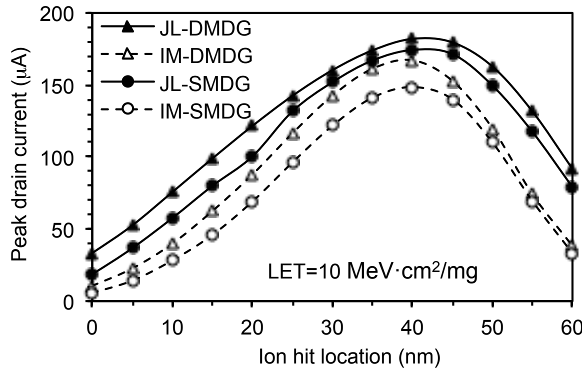

Fig. 6. Peak of the drain current transient as a function of the ion hit location (LET=10 MeV.cm^2/mg).

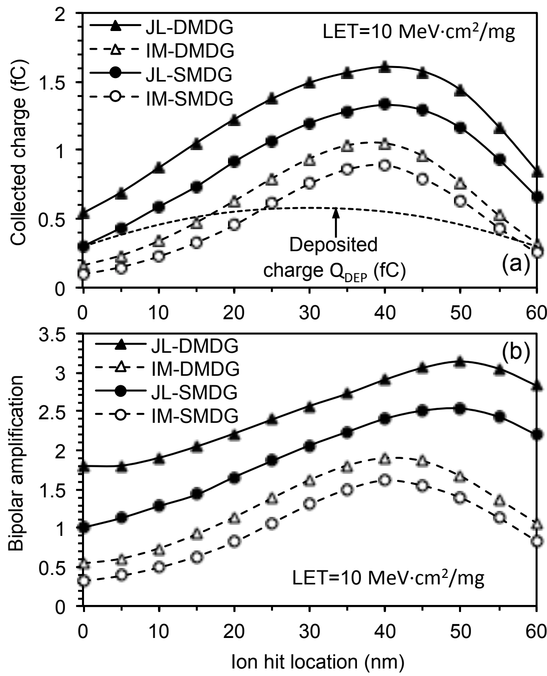

Fig. 7. Collected charge and bipolar gain as a function of the ion hit location (LET=10 MeV.cm^2/mg).

5. Impact of technological parameters on transient response of JL-DMDG devices

We also investigated the impact of several technological parameters on the transient response of JL-DMDG. Simulations have been performed on dual-material-gate devices with various lengths of the high-gate workfunction region, L_1, in order to evaluate the impact of this parameter on the transient response of JL-DMDG devices. Figure 8 plots the bipolar gain obtained in DMDG devices as function of L_1. The simulation results indicate that the bipolar amplification increases when the length of high-gate

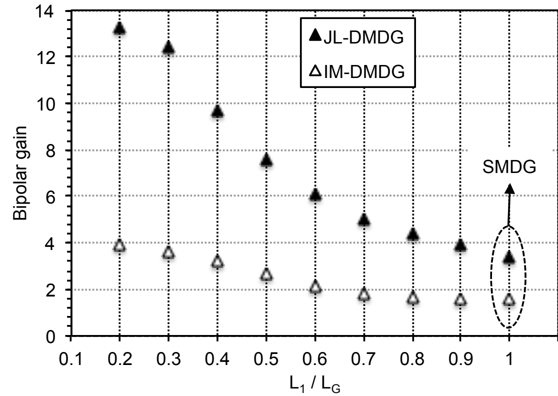

Fig. 8. Bipolar gain as function of the length of the high-gate workfunction region, L1, for LET=1 MeV.cm^2/mg in DMDG devices (the ion hit location is x=30 nm).

workfunction region is reduced. The JL-DMDG structures with $L_1>0.8\times L_G$ have bipolar gains close to that of the JL-SMDG structure, which is very interesting for obtaining hardened JL-DMDG devices. We also vary the metal-gate M2 workfunction in JL-DMDG devices and investigate its influence on the bipolar gain. These additional simulations and a detailed discussion will be included in the full paper.

References

[1] J.T. Park, J.P. Colinge, IEEE Trans. Electron Devices, vol. 49, no. 12, pp. 2222-2229, 2002.

[2] C.-W. Lee et al., Applied Physics Letters 94 (2009) 053511.

[3] J.P. Colinge et al., Nature Nanotechnology 5 (2010).

[4] W. Long, H. Ou, J.-M. Kuo, K.K. Chin, IEEE Trans. Electron Devices, vol. 46, no. 5, pp. 865-870, 1999.

[5] T.K. Chiang, Microelectronics Reliability, vol. 49, pp. 693-698, 2009.

[6] G.V. Reddy, M.J. Kumar, IEEE Trans. Nanotechnol., vol. 4, pp. 260–268, 2005.

[7] J. Singh, V. Gadi, and M. J. Kumar, IEEE Trans. Electron Devices, vol. 63, no. 6, pp. 2282-2287, 2016.

[8] P. Wang, Y. Zhuang, C. Li, Y. Li, and Z. Jiang, Jpn. J. Appl. Phys., vol. 53, no. 8, p. 084201, 2014.

[9] D. Munteanu, J.L. Autran, Microelectronics Reliability, vol. 55, pp. 1522-1526, 2016.

[10] D. Munteanu, J.L. Autran, Microelectronics Reliability, vol. 54, pp. 2284-2288, 2014.

[11] D. Munteanu, V. Ferlet-Cavrois, J.L. Autran, P. Paillet, J. Baggio, O.Faynot, C. Jahan, L. Tosti, IEEE Trans. Nucl. Sci., vol. 53, no. 6, pp. 3363-3371, 2006.

[12] M. Vinet et al., IEEE Electron Dev. Lett., vol. 26, pp. 317-319, 2005.

[13] Synopsys Sentaurus TCAD tools, Available online: http://www.synopsys.com/products/tcad/tcad.html.

[14] Y.P Fang, A.S. Oates, IEEE Trans. Device and Material Reliability, vol. 11, pp. 551-554, 2011.